

## The PLD Method Enhances the Surface Properties of 316 and 304 Stainless Steel by Coating ZnO Films

Sarah A. Jasim<sup>1\*</sup>, Ammar A. Habeeb<sup>1</sup>, A. Kadhim<sup>2</sup>

<sup>1</sup>Department of Physics, College of Science, Diyala University, Iraq

<sup>2</sup>Laser & Optoelectronics Engineering Department, University of Technology, Iraq

\*Corresponding author: sarahmaster91@gmail.com

### Abstract

This study employed two alloys of AISI (316,304) Stainless steel to improve the mechanical characteristics. In addition, the corrosion rate achieved by pulse laser deposition (PLD) can be reduced by applying a ZnO coating. Zinc oxide has garnered significant interest. Biomaterials have long been well-acknowledged for their use in dentistry and medical applications. Using an optical microscope examined the coating morphology, scanning electron microscopy (SEM), and energy-dispersive X-ray spectroscopy (EDS). The corrosion protection has been examined by assessing the mechanical characteristics when submerged in saliva with a pH of 5.6. The surface alteration is assessed using roughness and microhardness measurements. The corrosion resistance of all samples is superior to that of bare AISI (316, 304) stainless steel.

### Keywords

Dentist's Alloys, PLD, Zinc Oxide, FE-SEM, EDS

Received: 21 September 2023, Accepted: 24 November 2023

<https://doi.org/10.26554/ijmr.20231314>

### 1. INTRODUCTION

To balance high mechanical resistance and resistance to environmentally induced corrosion in standard atmospheres, stainless steels like 316 and 304 are widely used (Redkina et al., 2020; Saboori et al., 2019). The substrate is insulated by a nanometric layer of chromium oxide that acts as a ceramic barrier coating, providing an insulating ability. This is made possible by a nanometric layer of chromium oxide acting as a ceramic barrier coating (Kumar and Acharyya, 2019; Weisenburger et al., 2011). Stainless steels are known for their protective layer that exhibits self-healing ability. The layer is composed of chromium oxide and can be re-formed spontaneously in the presence of oxygen if it is removed or scratched away. However, in highly aggressive environments that contain  $\text{Cl}^-$  and/or  $\text{S}_2^-$  ions, stainless steels may not have sufficient corrosion resistance, especially at high temperatures or extreme pH levels above 12 or below 2 (Andrei et al., 2019; Sánchez-Tovar et al., 2012).

Mouth metals must not produce harmful corrosion products; even safe metals can create toxic compounds (Phillips, 1973). It is worth mentioning that the mouth is an ideal environment for the formation of corrosion products. The oral cavity is always moist and exposed to temperature changes. Our food and drinks have varying pH ranges, which can release acids during digestion. As a result, food particles tend to cling tightly to metallic restorations, creating a concentrated area that is highly conducive to an

accelerated chemical reaction between the metal or alloy and the oral environment (Duffo and Castillo, 2004). Saliva is vital for testing dental materials. Corrosion can be minimized by using modern alloys, thin films, and coatings on the metal surface (Xu et al., 2014). Pulsed Laser Deposition (PLD) is a technique used to deposit unique materials (thin films) onto a substrate. In this process, a high-power pulsed laser is used to focus on the desired target in a vacuum chamber. PLD process offers several benefits over other techniques, such as spray welding or plating, as it gives a stronger metallurgical bond with less heat input and minimum dilution. The PLD process is also highly controllable and produces a low Heat Affected Zone (HAZ) (Aperador et al., 2016). Nanomaterials can enhance active corrosion protection in coatings, prolonging their lifetime. They are effective inhibitors due to their high efficiency, low cost, low toxicity, and ease of production (Shen et al., 2014). Nanoparticles have an advantage in protecting materials against corrosion. Due to their small size, they have a larger surface area, which increases the number of surface atoms and enhances their physical, mechanical, and physicochemical resistance (Fedel and Deflorian, 2016). Zinc oxide's high biocompatibility and fast electric transfer kinetics make it suitable for use as a biomimetic membrane to immobilize and modify biomolecules (Jin et al., 2009). In many literatures, it can be learned that nano ZnO offers better performance than bulk ZnO. Zinc is a necessary element for our health. Additionally, ZnO nanoparticles have good biocompatibility with human

cells (Singh et al., 2013). Metal and its oxide nanoparticles are effective in controlling corrosion. They can be easily applied as a corrosion inhibitor on metallic surfaces. Many researchers have reported that the adsorption of metal nanoparticles and their oxides on metal surfaces can offer a corrosion inhibition phenomenon. Recent reports have shown that using metal and their oxide nanoparticles, such as  $\text{Cu}_2\text{O}$  and  $\text{ZnO}$ , can improve corrosion resistance (Hasnidawani et al., 2017),  $\text{ZrO}_2$ ,  $\text{SiO}_2$  (Wu et al., 2014).

## 2. EXPERIMENTAL SECTION

### 2.1 Materials

Zinc nitrate  $\text{Zn}[\text{NO}_3]_2 \cdot 6\text{H}_2\text{O}$  with purity of (99%) from THOMAS BAKER company / India. Double distilled water were the materials employed in this study and ammonia solution 25%  $\text{NH}_4\text{OH}$ .

### 2.2 Samples Preparation

We used tempered steel composites (316, 304) cut into round structures with a width of 20mm and a thickness of 5mm. The metallography was used to clean the samples, cleaning papers, and  $\text{Al}_2\text{O}_3$ . Each sample was mounted using EPOXY material (A:B) and solidified for 30 minutes. The samples were punched, wired, and inspected using an ovometer instrument before the erosion began. Figure (1) shows the final look of the samples.



Figure 1. Preparation Alloys for Corrosion Test

### 2.3 Preparation of Zinc Oxide Nanoparticles (ZnO-NPs)

We prepared zinc oxide nanoparticles (ZnO-NPs) in our experiment using the co-precipitation method. To do this, we added 11.9 g of zinc nitrate to 150 mL of double distilled water and continuously stirred until the zinc nitrate was completely dissolved. We then slowly added  $\text{NH}_4\text{OH}$  solution (%25) drop by drop and constantly stirred with a magnetic stirrer until the pH reached 11, which resulted in a white solution. Afterward, we washed the nano zinc oxide twice with double distilled water to remove any by-products and dried it at  $140^\circ\text{C}$  in a hot oven.

Finally, the ZnO nanoparticles were calcinated in the oven at  $550^\circ\text{C}$  for 2 hours (Alwan et al., 2015). In the experiment depicted in Figure (2), I utilized artificial saliva to conduct the corrosion test. To achieve the desired pH level similar to that of human saliva (5.6), I added HCl acid. It is worth noting that human saliva's pH level is associated with various health conditions. Some examples of chronic diseases include cancer, diabetes, high blood pressure, and kidney disease. Diseases. Moreover, the pH level of saliva varies with age, with adults having more acidic saliva than children. Food and drink intake can also modify the pH level of saliva (Meyer and Nally, 1975).

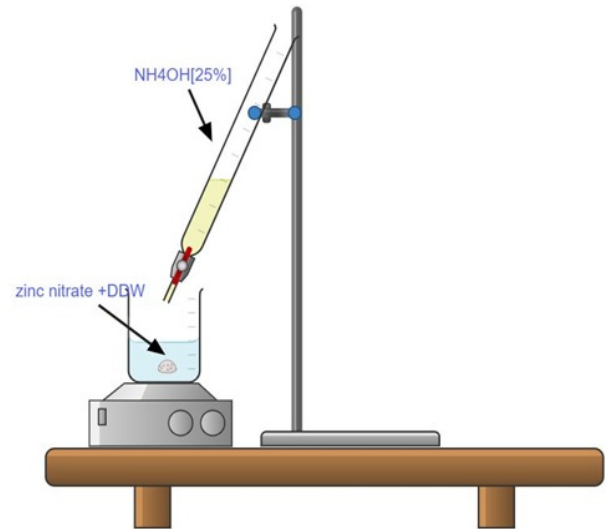


Figure 2. Preparation of ZnO NPS

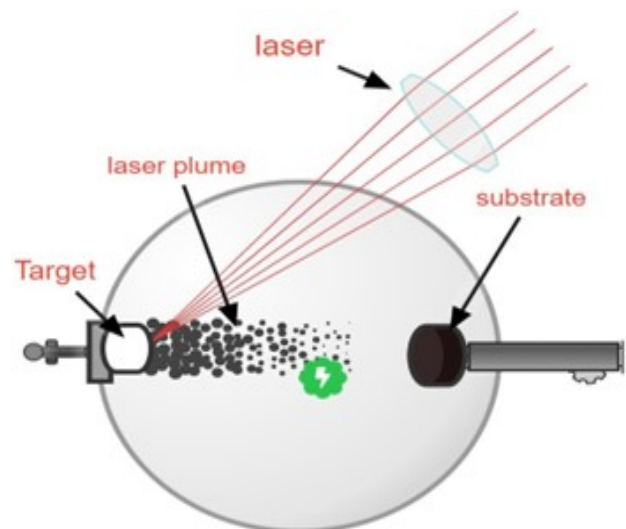


Figure 3. Set Up of Pulsed Laser Deposition (PLD) System

### 2.4 Chemical Compositions of Alloys

The chemical composition of the samples was analyzed using SPECTRO MAXx Instruments provided by AMETEK Materials

Analysis. The results of the analysis are displayed in Table 1. Let me know if you want me to modify it further. It can be found on the Ministry of Planning's Central Organization for Standardization and Quality Control website.

**2.5 Pulse Laser Deposition (PLD)**

Let me clarify the details of the PLD system for you. It comprises several crucial components, such as an Nd: YAG laser, a deposition chamber, a target, a substrate, a substrate heater, and a vacuum system. You can find a schematic diagram of all these parts of the PLD system in Figure (3). Various conditions were altered and documented throughout the process in Table (2). The PLD process was conducted at the Postgraduate Laboratory in the Laser and Optoelectronics Engineering Department at the University of Technology.

**2.6 Corrosion Test**

A Digi-ivy, Inc. potentiostat/galvanostat (DY2323) operated by a computer was used to take the voltammetric measurements in the Figure (4). The durability of the coatings was assessed in terms of their corrosion resistance. In a saliva solution at room temperature that was not stirred and had a pH of (5.6). The cell comprises three electrodes: a reference electrode made of Ag/AgCl, a counter electrode made of platinum wire, and a working electrode made of samples (304, 316) SS (Aperador et al., 2016). With the aid of an appropriate sticky polymer and just 1.0 cm<sup>2</sup> of their surface coming into touch with the solution, samples are shielded against crevice corrosion. The potential range beginning at around 4000 mV was measured using linear sweep voltammetry at a scan rate of 0.1 V/s. To determine specific electrochemical properties, we utilized the Tafel extrapolation method for calculation. The corrosion current density (color), polarization resistance (Rp), and other experimental data using the Corrosion Test Software (Hasnidawani et al., 2017).

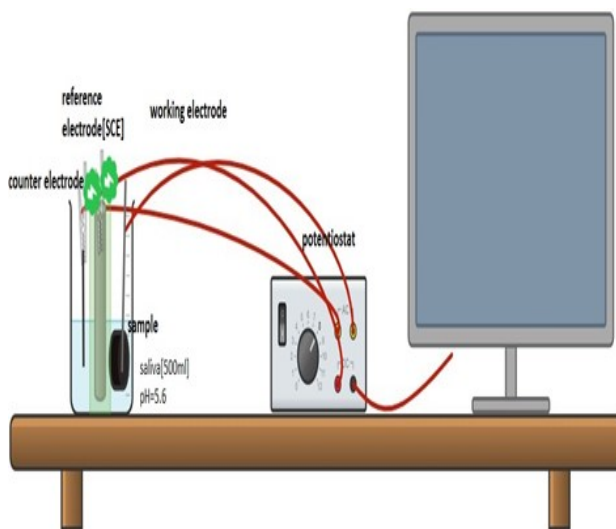


Figure 4. Sketch of Corrosion Test

**3. RESULTS AND DISCUSSION**

**3.1 X-Ray Diffraction**

The X-ray diffraction results indicate that the material produced at a temperature of 550°C is a ZnO nanoparticle. The spectra show ZnO's typical hexagonal wurtzite structure, as per the standard card (JCPDS No. 79-0208). The matching diffraction peaks at 2θ of 36.50°, 32.01°, and 34.67° correspond to (100), (002), and (101) planes, respectively. Figure (5) displays ZnO powder shows a crystalline, hexagonal structure through X-ray diffraction patterns. The crystallinity of ZnO improves after annealing at 550°C, as indicated by sharper and higher peak intensities in the annealed ZnO sample identified through standard data (Baruah and Dutta, 2009). The Debye-Sherrer Equation (1) was used to estimate the mean size of the as-prepared ZnO nanoparticles, around 28 nm (Lupan et al., 2010).

$$D = \frac{K\lambda}{\beta \cos \theta} \tag{1}$$

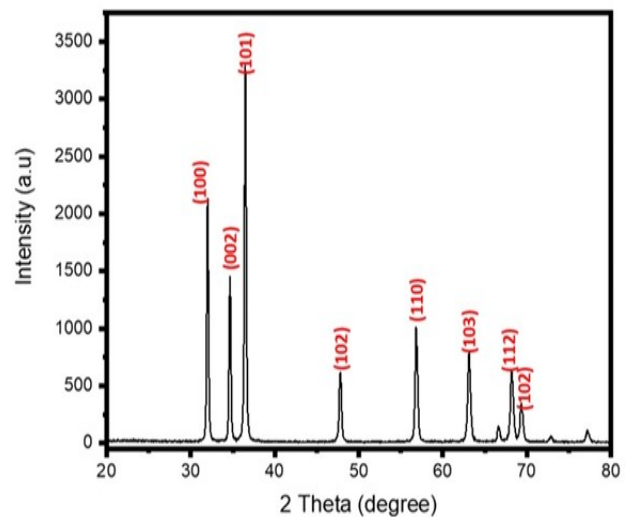


Figure 5. This Image Displays the X-Ray Diffraction Patterns of the ZnO Powder

**3.2 Micro-Hardness**

The microhardness of dental alloys (316, 316) stainless steel was measured using the Microhardness method before and after coating them with ZnO. Pulse laser deposition (PLD) processing was conducted under fixed conditions, as per Table 3. Before ZnO coating, the alloys had a microhardness value of about 200 HV. After ZnO coating processing, the measurements ranged from 295.8 HV to 335.8 HV for (304, 316) SS, respectively. The primary reason for improving microhardness is the solution's strengthening effect containing the ZnO element (Baruah and Dutta, 2009).

**Table 1.** Chemical Composition of 316 and 304 Stainless Steel (wt%)

Composition	C	Cr	Ni	Mn	Mo	Si	P	S	N	Co	Fe
316(wt%)	0.049	16.817	10.02	1.109	2.093	0.454	0.029	0.001	0.005	0.205	base
Composition	C	Si	Mn	P	S	Cr	Ni	Al	Cu	Fe	
304(wt%)	0.065	0.262	1.48	0.0269	0.420	17.93	8.71	0.0046	0.436	Bal.	

**Table 2.** Film Deposition Parameters

Parameters	Type and/or size	
Material	Target	ZnO nanoparticles
	Substrate	316, 304 stainless steel
Laser parameter	Wavelength [nm]	1064
	Repetition rate [Hz]	3
	Energy [mJ]	1000
	Pulse number [shot]	500
	Pulse width [ns]	10
Pressure parameter	Base pressure [mbar]	10 <sup>-2</sup>
Target parameter	Diameter [cm]	2
	Thickness [cm]	0.5
Substrate parameter	Area [cm <sup>2</sup> ]	3.14
	Thickness [cm]	0.5
	Temperature [C]	200°
Distance between	Contact (L) [cm]	12

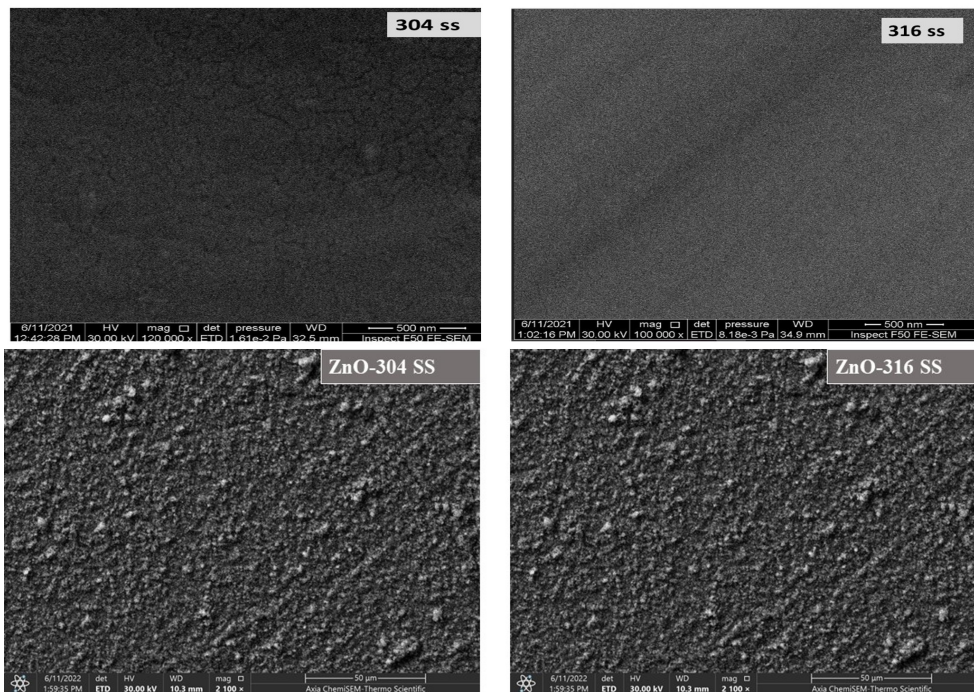


**Figure 6.** The SEM of Alloys (316, 304) Stainless Steel Surface Before and After Applying ZnO Coating by PLD

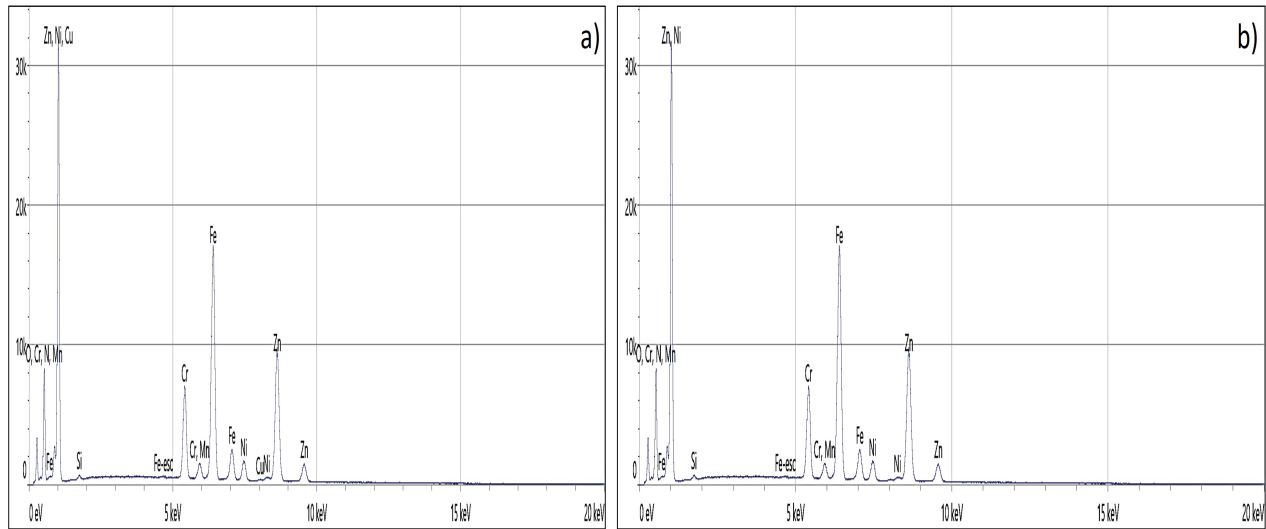


Figure 7. The EDS of Alloys (304 (a), 316 (b)) Stainless Steel Surface After Applying ZnO Coating by PLD

Table 3. The Result of Micro Hardness and Roughness

	ZnO-316 SS		ZnO-304 SS	
Micro-hardness	200	335.8	200	295.8
Roughness	0.039	0.284	0.03	0.144

3.3 Surface Roughness

The study measured the surface roughness of dental alloys, namely stainless steel 304 and 316, before and after coating them with ZnO through pulse laser deposition (PLD) processing. The initial surface roughness value was Ra= 0.03 nm before applying the ZnO coating. However, after the coating process, the surface roughness value increased to 0.144 nm for 304 SS alloy and 0.284 nm for 316 SS alloy. The findings are presented in Table 3 (Baruah and Dutta, 2009).

3.4 SEM and EDS Measurement

SEM images of the surfaces of 316 and 304 stainless steel samples treated with ZnO coating using PLD are displayed in Figure (6). The Figure displays the surface of the (304,316) SS alloy and the crystallites formed by ZnO coating on 316 and 304 alloys. The applied treatments resulted in better corrosion performance. Coated samples have a smooth, defect-free surface. Figure (7) shows the uniform distribution of Zn, O, and Fe elements on 304 and 316 stainless steel samples treated with ZnO coating. O distribution follows the Zn distribution, indicating the formation of Zn oxide in both samples (Baruah and Dutta, 2009).

3.5 FE-SEM Measurement

The morphology of ZnO nanoparticle coating on 304 and 316 stainless steel samples was studied using pulsed laser deposition (PLD) and field emission scanning electron microscopy (FE-SEM). FE-SEM images of the ZnO nanoparticle coatings on 304 and 316 stainless steel are presented in Figures 8a and b, respectively.

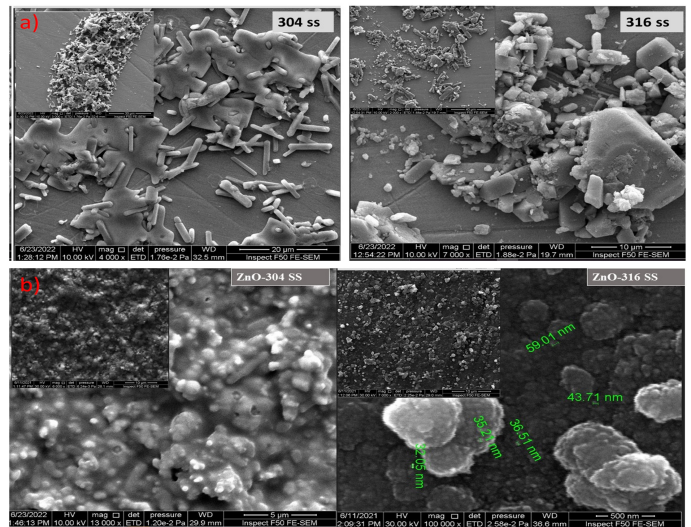
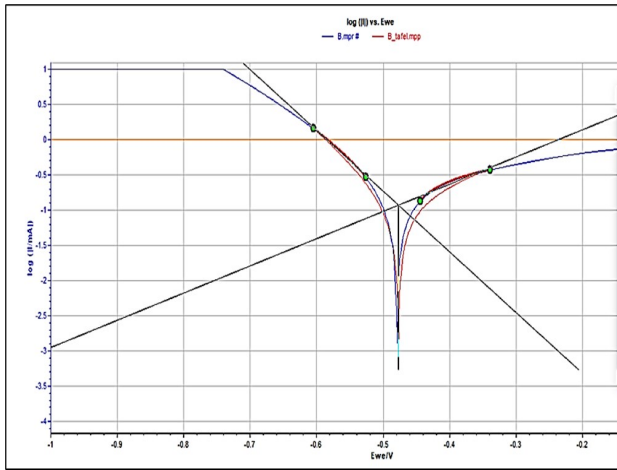


Figure 8. The FE-SEM Images of 304, 316 Stainless Steel, Respectively (a), and the ZnO Nanoparticles Coating on 304-316 Stainless Steel After the Corrosion Test (b)

Before the ZnO coating, the surfaces of the alloys were rough and showed cracks due to agglomeration of the ZnO nanoparticles, resulting in surface corrosion. Figure 8b shows that the surface of alloys with ZnO coatings have uniform dispersion and are homogeneously distributed all over the surface with only a few agglomerations. Additionally, the coatings exhibit a smooth surface with no apparent cracks or other defects. In comparison, 316 stainless steel alloys with ZnO coating were found to have better inhibitors than 304 stainless steel alloys with ZnO coating because they did not show pitting corrosion on their surface (Samad et al., 2018).

**Table 4.** Corrosion Parameters of Untreated 316, 304 SS Alloys in a Artificial Saliva at 37°C

	I <sub>corr</sub> ( $\mu\text{A}/\text{cm}^2$ )	E <sub>corr</sub> (mV)	b <sub>a</sub> (mV/dec)	b <sub>c</sub> (mV/dec)	R <sub>p</sub> ( $\text{k}\Omega.\text{cm}^2$ )	Efficiency %
Zno-304	69.07	-747.47	134.6	112.8	0.69	41
ZnO-316	8.14	-923.33	110.8	146.5	0.081	95



**Figure 9.** Tafel Plot of 316 SS Alloy Before PLD

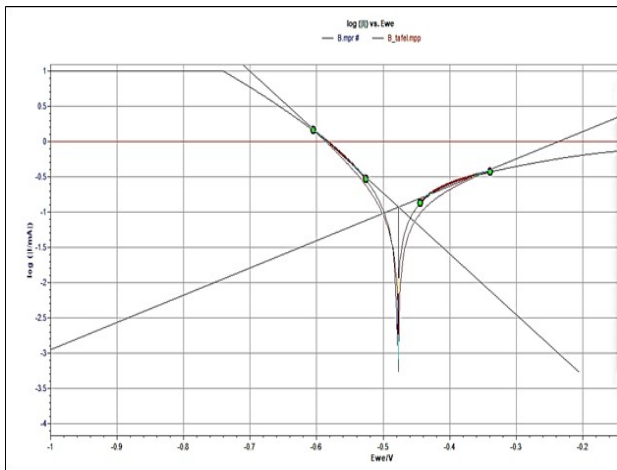


**Figure 10.** Tafel Plot of 304 SS Alloy Before PLD

**3.6 Corrosion Tests Results**

The surface treatment that is used to study its effect on corrosion resistance nanoparticle coating (ZnO) on stainless steel alloys. The circumstances accompanying this process are listed in Table 4 and Figures (9-12). Table (4) presents the polarization behavior of two dental alloys treated in artificial saliva at pH= 5.6 and 37°C. The results indicate that the polarization curves consist of two regions: the anodic region (upper section of the curve), where metals or oxidation dissolve. Sometimes, the presence of these acidic saliva yields increases the dissolution of metals in 316,304 alloys to take a wide range of potentials in the anodic

region. It is possible to observe the corrosion current densities. They have higher values, and 316 SS alloys were more effective than 304 SS alloys in decreasing corrosion current density after nanoparticle coating (ZnO). On the other hand, nanoparticle coating (ZnO) treatment for the two dental alloys gave a width in the passive region. The polarization behavior of treated alloys in the presence of nanoparticle coating (ZnO) in artificial saliva shows more corrosion potential. The corrosion rate for treated ZnO nanoparticles decreased in saliva solutions (Samad et al., 2018).

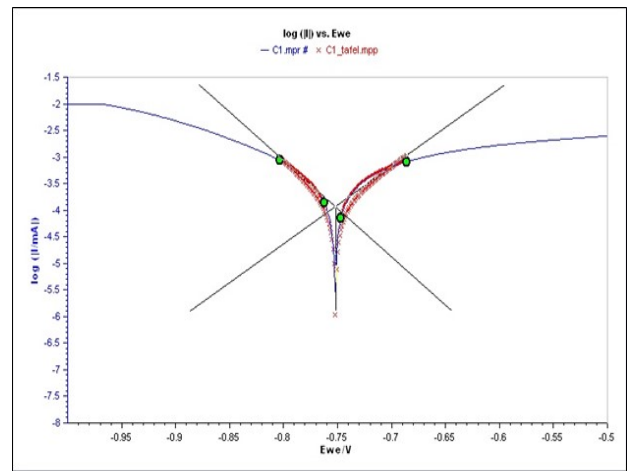


**Figure 11.** Tafel Plot of ZnO-316 SS Alloy by PLD

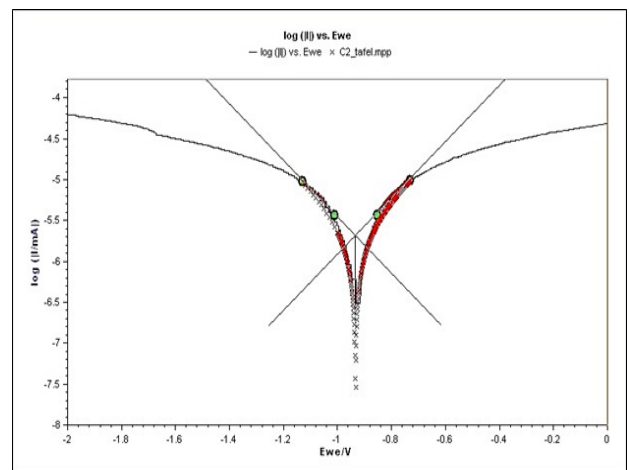


**Figure 12.** Tafel Plot of ZnO-304 SS Alloy by PLD

#### 4. CONCLUSION

Dental alloys of 316 and 304 stainless steel are known for their excellent corrosion resistance properties. However, patients with diseases that affect the pH level of their saliva, such as cancer, diabetes, high blood pressure, kidney diseases, etc., may experience raised acidic mouth liquid, which can lead to corrosion of dental alloys. In such cases, coatings with ZnO by pulsed laser deposition (PLD) can be beneficial in improving the corrosion behavior of dental alloys. Food and drink can also change the pH level of saliva, and age may also play a role. Adults, for instance, tend to have more acidic saliva than children. Coating dental alloys with ZnO can improve their mechanical properties and corrosion behavior. The treated samples exhibit lower corrosion current values than the untreated samples. The deposition of ZnO films reduces the corrosion currents. ZnO nanoparticles ceramic synthesized using co-precipitation can effectively coat dental alloys. The XRD spectrum shows the hexagonal structure of ZnO annealed at 550°C. The microhardness and roughness of dental alloys increase with ZnO coating. SEM images show that the morphology of surface particles changes to a sphere-like shape, and corrosion decreases in dental alloys with ZnO coating. The FE-SEM image reveals that dental alloys have a pH of 5.6 when immersed in saliva. Dental alloys with ZnO coating offer better protection, and the corrosion ratio is lower than without. Dental alloys with ZnO coating also exhibit different surface corrosion types, such as general corrosion and pitting corrosion. Compared to 304 SS, alloys 316 SS with ZnO coating are better.

#### 5. ACKNOWLEDGEMENT

We would like to thank College of material Engineering, technology University for to help me with the measurements. And for the structure properties analysis.

#### REFERENCES

- Alwan, R. M., Q. A. Kadhim, K. M. Sahan, R. A. Ali, R. J. Mahdi, N. A. Kassim, and A. N. Jassim (2015). Synthesis of Zinc Oxide Nanoparticles Via Sol-Gel Route and Their Characterization. *Nanoscience and Nanotechnology*, **5**(1); 1-6
- Andrei, V. A., V. Malinovski, C. Radulescu, I. Ionita, G. Torok, E. Coaca, A. H. Marin, and G. Bokuchava (2019). Applications of Plasma Electrolytic Saturation Technique in the Field of Nuclear Materials. *Journal of Science and Arts*, **1**; 185-194
- Aperador, W., J. Bautista-Ruiz, and E. Delgado (2016). Hot Corrosion Resistance of Al<sub>2</sub>O<sub>3</sub> Coating Produced by Thermal Spray. *International Journal of Electrochemical Science*, **11**; 9424-9437
- Baruah, S. and J. Dutta (2009). Hydrothermal Growth of ZnO Nanostructures. *Science and Technology of Advanced Materials*, **10**(2009); 013001
- Duffo, G. and E. Q. Castillo (2004). Development of an Artificial Saliva Solution for Studying the Corrosion Behavior of Dental Alloys. *Corrosion*, **60**(6); 594-602
- Fedel, M. and F. Deflorian (2016). Electrochemical Characterization of Atomic Layer Deposited Al<sub>2</sub>O<sub>3</sub> Coatings on AISI 316L Stainless Steel. *Electrochimica Acta*, **203**; 404-415
- Hasnidawani, J., N. A. Hassan, H. Norita, N. Samat, N. N. Bonnia, and S. N. Surip (2017). ZnO Nanoparticles for Anti-Corrosion Nanocoating of Carbon Steel. In *Materials Science Forum*, volume 894. Trans Tech Publ, pages 76-80
- Jin, T., D. Sun, J. Su, H. W. Zhang, and H. J. Sue (2009). Antimicrobial Efficacy of Zinc Oxide Quantum Dots against *Listeria monocytogenes*, *Salmonella enteritidis*, and *Escherichia coli* O157: H7. *Journal of Food Science*, **74**(1); M46-M52
- Kumar, P. S. and S. Acharyya (2019). Controlling Chloride Induced Stress Corrosion Cracking of AISI 316L Stainless Steel by Application of Buffing. *Materials Today: Proceedings*, **15**; 138-144
- Lupan, O., T. Pauporté, L. Chow, B. Viana, F. Pellé, L. K. Ono, B. R. Cuenya, and H. Heinrich (2010). Effects of Annealing on Properties of ZnO Thin Films Prepared by Electrochemical Deposition in Chloride Medium. *Applied Surface Science*, **256**(6); 1895-1907
- Meyer, J. and J. Nally (1975). Influence of Artificial Salivas on Corrosion of Dental Alloys. In *Journal of Dental Research*, volume 54. pages 678-678
- Phillips, R. W. (1973). Skinner's Science of Dental Materials. W. B. Saunders Company, XII+682, 26x18 cm, Illustrated, 1973
- Redkina, G., A. Sergienko, and Y. I. Kuznetsov (2020). Hydrophobic and Anticorrosion Properties of Thin Phosphonate-Siloxane Films Formed on a Laser Textured Zinc Surface. *International Journal of Corrosion and Scale Inhibition*, **9**(4); 1550-1563
- Saboori, A., A. Aversa, F. Bosio, E. Bassini, E. Librera, M. De Chirico, S. Biamino, D. Ugues, P. Fino, and M. Lombardi (2019). An Investigation on the Effect of Powder Recycling on the Microstructure and Mechanical Properties of AISI 316L Produced by Directed Energy Deposition. *Materials Science and Engineering: A*, **766**; 138360
- Samad, U. A., M. A. Alam, A. Chafidz, S. M. Al-Zahrani, and N. H. Alharthi (2018). Enhancing Mechanical Properties of Epoxy/polyaniline Coating with Addition of ZnO Nanoparticles: Nanoindentation Characterization. *Progress in Organic Coatings*, **119**; 109-115
- Sánchez-Tovar, R., M. Montañés, J. Garcia-Anton, and A. Guenbour (2012). Influence of Temperature and Hydrodynamic Conditions on the Corrosion Behavior of AISI 316L Stainless Steel in Pure and Polluted H<sub>3</sub>PO<sub>4</sub>: Application of the Response Surface Methodology. *Materials Chemistry and Physics*, **133**(1); 289-298
- Shen, Y., X. Guo, Y. Lin, and J. Tao (2014). Al<sub>2</sub>O<sub>3</sub> Coatings Fabricated on Stainless Steel/Aluminium Composites by Microarc Oxidation. *Surface Engineering*, **30**(10); 735-740
- Singh, P., O. Sinha, R. Srivastava, A. Srivastava, S. V. Thomas, K. Sood, and M. Kamalasanan (2013). Surface Modified ZnO Nanoparticles: Structure, Photophysics, and Its Optoelectronic Application. *Journal of Nanoparticle Research*, **15**; 1-9
- Weisenburger, A., C. Schroer, A. Jianu, A. Heinzl, J. Konys, H. Steiner, G. Müller, C. Fazio, A. Gessi, and S. Babayan (2011). Long Term Corrosion on T91 and AISI 316L Steel in Flowing Lead Alloy and Corrosion Protection Barrier Development:

- Experiments and Models. *Journal of Nuclear Materials*, **415**(3); 260–269
- Wu, L. K., X. F. Zhang, and J. M. Hu (2014). Corrosion Protection of Mild Steel by One-Step Electrodeposition of Superhydrophobic Silica Film. *Corrosion Science*, **85**; 482–487
- Xu, P., C. Lin, C. Zhou, and X. Yi (2014). Wear and Corrosion Resistance of Laser Cladding AISI 304 Stainless Steel/ $\text{Al}_2\text{O}_3$  Composite Coatings. *Surface and Coatings Technology*, **238**; 9–14